THE JOURNAL OF PHYSICAL CHEMISTRY B

Article

pubs.acs.org/JPCB

Bromide Ion Exchange with a Keggin Polyoxometalate on Functionalized Polymeric Membranes: A Theoretical and Experimental Study

G. De Luca,*[,†] F. Bisignano,[†] A. Figoli,[†] F. Galiano,[†] E. Furia,[‡] R. Mancuso,[‡] O. Saoncella,[§] M. Carraro,[§] M. Bonchio,[§] and B. Gabriele[‡]

[†]Research Institute on Membrane Technology (ITM-CNR), University of Calabria, Via P. Bucci, I-87036 Arcavacata di Rende (CS), Italy

[‡]Department of Chemistry and Chemical Technologies, University of Calabria, Via P. Bucci, I-87036 Arcavacata di Rende (CS), Italy

[§]Department of Chemical Sciences and ITM-CNR, University of Padova, Via Marzolo, 1, 35131 Padova, Italy

ABSTRACT: Noncovalent interactions between the polyoxometalate $[PMo_{12}O_{40}]^{3-}$ and acryloyloxyundecyltrimethyl ammonium bromide surfactant, used during membrane preparation, were evaluated in the frame of density functional theory. The electronic solvation energy of $[PMo_{12}O_{40}]^{3}$ and bromide anions was also evaluated, at the same level of theory, in order to predict a probable exchange on the polymeric surface between these anions at the water/polymer interface. Energy balances were theoretically assessed, showing that the bromide cannot be exchanged with this nanosized polyanion in large extent. In order to validate this theoretical conclusion, *ad hoc* and accurate measurements were carried out by using homemade polymeric membranes and by dipping them in an ca. 0.4 mM solution of $Na_3[PMo_{12}O_{40}]$ for 4 days. The Br^- concentration, released in a polyoxometalate solution, was followed at different times during the test period by gravimetrical analysis. The agreement between the theoretical prediction and experimental data was remarkable, as the quantum calculations correctly accounted for the short-range intermolecular interactions involved in this phenomenon. Bearing in mind that the achieved conclusion is based on an *ab initio* quantum approach, the findings of this study can be considered rather general and then exploitable for other similar systems.

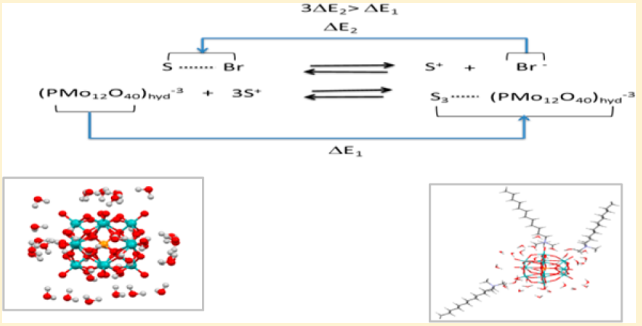

1. INTRODUCTION

The exchange of ions on a polymeric surface is a topic of considerable interest, thanks to the broad range of applications. In particular, the anion exchange on membrane surfaces may offer new possibilities for the development of novel functionalized membranes. In fact, polymeric surface modification by binding specific functional groups represents a widely used procedure for membrane preparation with peculiar functions.[1−6] Moreover, many studies have been devoted to the use of various additives, including nanoparticles, and specific coatings of existing membranes. Thus, target surface properties such as antimicrobial, catalytic activity and hydrophobicity can be imparted to the membranes. In this frame, innovative nanostructures would definitely make a leap forward. For example, the replacement of ions, without particular features, with functional nanosized polyanions may represent an efficient strategy for the design of novel polymeric membranes. Therefore, this work aims to describe noncovalent short-range interactions involved in the exchange, on a polymer surface, of the bromide with the polyoxometalate $[PMo_{12}O_{40}]^{3-}$.

Polyoxometalates (POMs) are polyanionic metal oxides and are widely used for the preparation of hybrid materials, owing to their large versatility in terms of tunable structural features and properties. Specifically, polyoxo vanadates and molybdates are promising antibacterial agents.[7,8] Their biological activity arises from the electrostatic interactions with biological molecules and from their redox behavior, which can be exploited for the oxidations of organic substrates[9] including cellular components.[10−14] In particular, the $[PMo_{12}O_{40}]^{3-}$ is a Keggin heteropolyanion with high redox potential, which has already been used for the preparation of antimicrobial films.[8] Thus, this Keggin heteropolyanion was used in this investigation.

Homemade membranes were prepared in this work by exploiting the polymerizable bicontinuous microemulsion (PBM) technique.[15−20] Polymerizable bicontinuous microemulsion is a general procedure used for the preparation of self-supported polymeric membranes. Cationic surfactants, such

Received: November 20, 2013
Revised: February 7, 2014
Published: February 18, 2014

as dodecyltrimethylammonium bromide (DTAB), cetyltrimethylammonium bromide (CTAB), and acryloyloxyundecyltrimethyl ammonium bromide (AUTMAB), have been used together with specific cosurfactants, monomers, cross-linkers, and water. The positive charged surfactants are typically outweighed by bromide ion, and the surfactant-bromide adduct is located in the aqueous phase of the bicontinuous microemulsion. Conversely, the monomers constitute the oily phase of the microemulsion. The bromide ion, linked to the positive charged heads of surfactants by noncovalent electrostatic interactions, may be exchanged with other water-soluble and functional anions (such as the Keggin heteropolyanion). In this way, the surfactants may be used as a hook to anchor nanoparticles on the surface of the polymeric membrane surface.

A computational and experimental study on the exchange of Br^- with the $[PMo_{12}O_{40}]^{3-}$ is presented in this work. A detailed theoretical analysis of the noncovalent interactions controlling the anion exchange was carried out. Following previous positive results,[21−24] describing hydrogen bonds in membranes (i.e., theory level[25−28] and geometric models), quantum mechanics (QM), in the frame of density functional theory (DFT), and molecular mechanics (MM) calculations were performed in this contribution. In particular, the MM simulations provided the most probable conformer of the AUTMAB surfactant which was used in the subsequent DFT calculations to assess accurately the interactions of the AUTMAB with the $[PMo_{12}O_{40}]^{3-}$ or Br^- anions. The electronic hydration energy of these anions were also evaluated, at the same level of theory. Finally, energy balances were carried out and the exchanging probability of Br^- with the $[PMo_{12}O_{40}]^{3-}$, at neutral pH, was predicted at qualitative level. The final aim of this work is to figure out whether a good adhesion of the nanosized metal oxide can occur on the functionalized polymeric surface without loss of the antibacterial activity. In fact, an efficient exchange, on the membrane surface, with antibacterial nanoparticles definitely allows the membrane's efficiency to be increased by reducing the fouling caused by microorganisms, particularly harmful during wastewater purification processes.

Finally, to validate the theoretical conclusions, *ad hoc* measurements were then carried out using homemade membranes in order to control the chemical composition of all the components involved in the exchange process. Analytical measurements were performed to assess the anionic exchange. The measurements are based on the gravimetrical analysis of the Br^- released in 4 days by the membrane as a consequence of the exchange with $[PMo_{12}O_{40}]^{3-}$ at neutral pH.[4]

2. EXPERIMENTAL SETUP

2.1. Membrane Preparation and Characterization. Bicontinuous microemulsions are formed at balanced conditions in which the oil (monomer) and the water domains are randomly dispersed in two phases, giving a sponge-like structure. Both phases are stabilized by the presence of the surfactant as well as of a cosurfactant that decreases the oil surface tension and allows a partial miscibility between the phases. Then, the bicontinuous microemulsions can be polymerized by addition of initiators, and the resulting latex is used as a membrane. A cross-linker is also normally added in order to strengthen the polymeric matrix. For the microemulsion preparation carried out in this work, methyl methacrylate (MMA) was used as monomer constituting the oily phase, 2-hydroxylethyl methacrylate (HEMA) was used as cosurfactant, while ethylene glycol dimethacrylate (EGDMA) was finally added as cross-linker. The polymerizable surfactant, AUTMAB, was synthesized according to literature data.[29] The ammoniumpersulfate and *N*,*N*,*N*′,*N*′-tetramethylethylenediamine were added as initiators in order to promote the polymerization. Conductivity measurements, in particular conductivity of the surfactant, at different aqueous concentrations, were carried out to identify the bicontinuous range. The conductivity data allowed the microemulsion type to be differentiated: water in oil W/O and oil in water O/W from bicontinuous microemulsions. Systems with a low conductivity (less than 8 mS/cm) designated W/O microemulsions. The bicontinuous range was defined by the increased conductivity observed upon water addition. A further addition of water brought the conductivity to decrease, designating the O/W microemulsion formation. On the basis of these results, the optimal PBM composition was found and reported in Table 1.

Table 1. Composition (wt %) of the Polymerizable Bicontinuous Microemulsion

MMA	HEMA	water	AUTMAB	EGDMA
21	10	41	25	3

Once the microemulsion was prepared, 20 mM initiators were added to the system. The microemulsion was, then, purged with nitrogen gas for about 1−2 min and poured in a glass Petri dish under nitrogen atmosphere where it was left to polymerize overnight.[30] The obtained membrane was washed several times before its use in order to remove the unreacted components. The bicontinuous structure was confirmed by scanning electron microscopy (SEM) analyses, as shown in Figure 1. PBM membrane presents the classic interconnected structure made up of an interconnected network of polymer channels (clear strips) and water channels (darker strips).

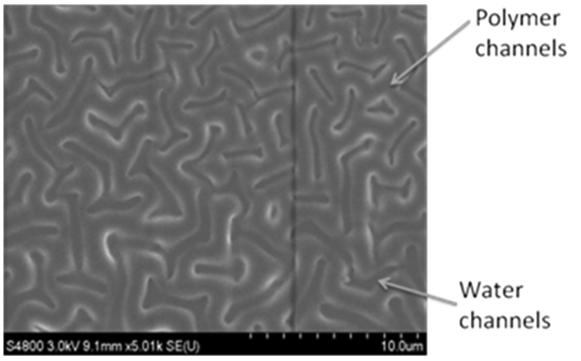

Figure 1. SEM surface of polymerizable bicontinuous microemulsion membrane.

2.2. Analytical Measurement of Ionic Exchange. The extent of the ionic exchange occurring on the membrane surface was assessed by gravimetrical analysis of the Br^- resulting from the exchange.[31,32] In detail, a solution of $[PMo_{12}O_{40}]^{3-}$ in distilled water (250 mL, ca. 0.4 mM) was prepared, and the membrane (Ø, ca. 1.5 cm) was dipped in the solution and allowed to stand in direct infusion for 96 h, while continuously stirring with a magnetic bar. In the picture reported in Figure 2, the experimental device used for the ionic exchange experiment was represented. A small amount (1 mL) of the solution was taken after 1, 5, 8, 24, 48, 72, and 96 h in

dx.doi.org/10.1021/jp411401v | J. Phys. Chem. B 2014, 118, 2396−2404

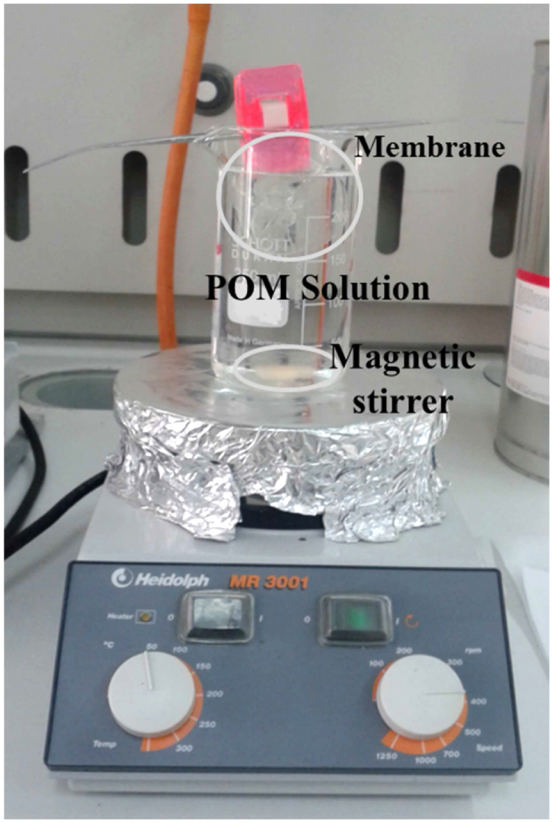

Figure 2. Experimental device used for the ionic exchange measurements.

order to determine the amount of Br^- released. The quantitative analysis of this anion was performed by adding to the solution (1 mL) an excess of 0.1 M $AgNO_3$ solution in distilled water. After precipitation of AgBr, the solid was filtered with the aid of porcelain crucibles, washed with the $AgNO_3$ solution, dried at 110 °C for 18 h, and weighed by an analytical balance with an accuracy of 0.0001 (g).

The $Na_3PMo_{12}O_{40}$ used for the ionic exchange measurements was obtained upon cation exchange of a $H_3PMo_{12}O_{40}$ solution on an Amberlyst resin, loaded with Na^+. In particular, the heteropolyacid was dissolved in water and eluted through a chromatographic column containing the Na^+ preloaded Amberlyst resin. Yellow/green soluble crystals of the product were obtained upon water removal under *vacuum*. The identity of the product was confirmed by ^{31}P NMR (δ = 0.5 ppm in D_2O) and by FT-IR. The $H_3PMo_{12}O_{40}$ was purchased from commercial sources (Sigma-Aldrich).

3. MOLECULAR MODELS AND COMPUTATIONAL DETAILS

The optimization of hydrated $[PMo_{12}O_{40}]^{3-}$ geometry and the AUTMAB conformational search were the first step of this work. The research of the surfactant's conformers has been carried out at MM level by using universal force field (UFF). The Avogadro software,[33] an application of the Open Babel platform,[34] was used for the conformational search. In Avogadro, a stochastic search method converging on low energy conformers by weighing molecular torsion angles based on the relative conformers' energies is implemented. The weighed rotor search method with a number of conformers equal to 100 has been applied 5 times, covering 500 possibilities, in order to obtain a sample of surfactant conformers. The most stable structure of this sample was then defined by subsequent quantum mechanics calculations. In particular, a Boltzmann distribution of the quantum energies of the optimized structures was taken into account[35] and the conformer with the highest Boltzmann factor was considered as preferred over the other structures. In Figure 3, the geometry of

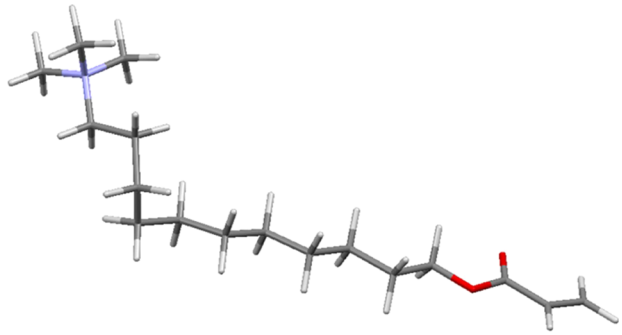

Figure 3. Most probable conformer of AUTMAB surfactant. Carbon atoms in gray color, oxygen atoms in red, nitrogen atom in blue, and hydrogen atoms in white.

the most probable AUTMAB conformer is reported, i.e., the surfactant with 11 atoms in the carbon chain, obtained by the illustrated procedure. The conformational analysis was carried out holding blocked the unsaturated group of the AUTMAB, used for the polymerization, in order to simulate the surfactant entrapment in the polymer matrix. Conversely, the polar head, represented by the positive ammonium polar head, $-N^+(CH_3)_3$, and the carbon chain were left completely free to move. The most stable conformer found is quite linear regardless of its carbon chain length, although the surfactant with 16 carbon atoms in the aliphatic chain (not reported here) is more twisted with respect to the AUTMAB. This preliminary analysis indicates that no special windings of the surfactants around the polyanionic nanoparticle should be expected, especially considering the AUTMAB with 11 carbon atoms.

After the conformational search, the number of water molecules around $[PMo_{12}O_{40}]^{3-}$ and their arrangement was evaluated. The assessment of the water disposition around POM is an important point for the subsequent calculations. Up to now, calculations on a similar large nanosystem have used mixed QM/MM approaches.[36−38] However, Miro et al.[38] recently studied, in detail, the hydration of similar Keggin anions analyzed through an explicit solvent model. The explicit solvent model, used by these authors, includes the molecules of water in the solvation shell explicitly and long-range bulk effects and counterions as a set of single point charges. Miro et al.[38] compared their results with those obtained by using the conductor-like screening model (COSMO),[39] finding a good agreement. A similar approach was used in this paper with the exception, with respect to Miro et al.'s work, that the long-range effects were taken into account by using the COSMO approach. Miro et al. showed that the number of hydrogen bonds between the water molecules and polyoxometalate significantly increase going from a first shell of 24 molecules to an outer shell of 49, whereupon these bonds between water and polyoxometalate remain nearly constant, whereas the H-bonds among water molecules significantly increase as well shown in Figure 2 of the Miro et al. paper.[38] Thus, here, 36 water molecules, i.e., an average value between the above first and

dx.doi.org/10.1021/jp411401v | J. Phys. Chem. B 2014, 118, 2396−2404

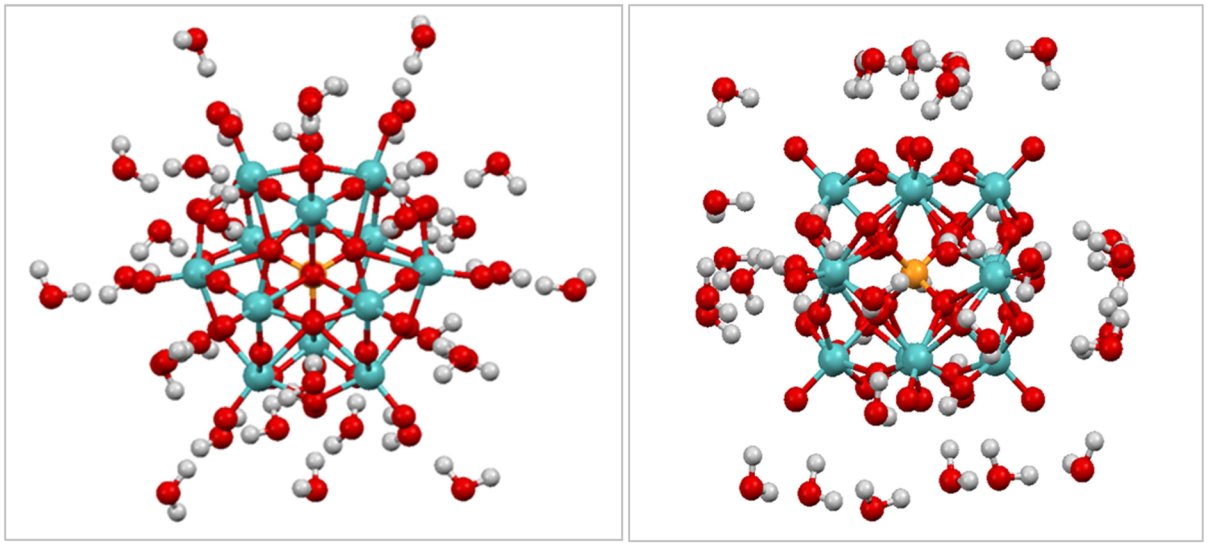

Figure 4. Initial (a) and DFT optimized geometries (b) of the hydrated $[PMo_{12}O_{40}]^{-3}$ (POM^{hyd}). Oxygen atoms in red color, molybdenum atoms in blue, hydrogen atoms in white, and phosphorus atom in yellow.

outer solvation shells, have been placed around the POM. It is worth noting that the optimization of the geometries of a number of water molecules greater than 36 by using a pure quantum mechanics method becomes prohibitively expensive. Every water molecule was bonded to each external POM oxygen atom by a typical H-bond distance,[40−43] and random dihedral angles were defined. As outlined above, a supra-molecular model is used in which the closest water molecules are explicitly considered, whereas all the other water molecules are taken into account by the COSMO model. It is important to consider that the supra-molecular structure, i.e., POM and 36 water molecules, allows the use of the bulk water dielectric constant, i.e., 80.2 in the COSMO calculations, preventing to take into account the nonlinear polarization effects of the dielectric constant when multicharged solutes are in solution. Moreover, the use of a pure quantum mechanics approach to describe the above supra-molecular structure guarantees a certain reliability of the results, mainly in relation to the hydrogen bonds formed by water with the POM. Thus, a full quantum optimization of all the water molecules was carried out using a hybrid energy functional, X3LYP,[44] whereas the polyoxometalate was kept stuck during the optimization. DFT calculations were performed using linear combinations of Gaussian-type orbitals, and the Coulomb and exchange-correlation potentials were numerically integrated on an adaptive grid with medium accuracy. Double-ζ orbital bases were employed for the phosphorus and internal oxygen atoms of the POM, instead, double-ζ orbital basis with a polarization function were employed for the external oxygen atoms and for water molecules. For the molybdenum atoms, the Stuttgart RSC 1997 effective core potentials were used. The energy convergence for the self-consistent field procedure and the root mean square of the electron density thresholds were set to 10^{-6} (a.u.) and to 2×10^{-5} (a.u.), respectively. The geometry was optimized by using analytical energy gradients and the quasi-Newton optimization with approximate energy Hessian updates. The convergence criteria for the geometry optimization are the maximum and root-mean-square gradient thresholds of 4.5×10^{-3} and 3.0×10^{-3}, respectively, in conjunction with the maximum and root-mean square of the nucleus Cartesian displacement vectors with thresholds of 5.4×10^{-3} and 3.6×10^{-3} (a.u.), respectively. As mentioned above, the COSMO solvent model, proposed by Klamt and Schüürmann,[39] was used to evaluate the electronic free energies of the hydrated POM and Br^-. The cavity, in which the hydrated anions, i.e., the supra-molecular structures, were located, is defined as interlocking atomic spheres constructed by using specific atomic radii. The default radii implemented in the NWChem package[45] were used. The use of these radii justifies the utilization of an "accessibility solvent parameter" for water molecules equal to 1.3 Å. In parts a and b of Figure 4, the initial and optimized geometries of the hydrated polyoxometalate are presented, respectively. In the geometry optimization of the hydrated nanoparticle (POM^{hyd}), it is evident that the water molecules move away from the POM oxygen's atoms, forming simultaneously molecular clusters with each other (Figure 4b). The most open structure of the hydrated anion allows some oxygen atoms to be identified on the $[PMo_{12}O_{40}]^{3-}$ surface which are less hindered by water. These atoms were afterward chosen to bind with the surfactant molecules. Conversely, the optimized hydrated POM allows to identify some parts of the POM surface more covered by the water molecules, i.e., water clusters, through which the nanoparticle could bind to the supports by means of H-bonds formed by water. These two possible attacks were then used to define the starting geometries of the POM^{hyd}–AUTMAB adducts for the next optimizations.

Finally, the energies associated with the noncovalent interactions between $[PMo_{12}O_{40}]^{3-}$ and AUTMAB as well between Br^- and surfactant (i.e., the ΔE_{int}) were evaluated as the difference between the energy of the adduct (anions and surfactants) and those of the isolated single components. The basis set superposition error was also included in the calculations of the interaction energies according to the counterpoise method.[46]

dx.doi.org/10.1021/jp411401v | J. Phys. Chem. B 2014, 118, 2396−2404

4. RESULTS AND DISCUSSION

The electrostatic long-range interactions, formed between a charged surface and the negatively charged nanoparticles, are weaker than short-range interactions;[47,48] however, this work was focused in the short-range electrostatic interactions involved in the anionic exchange. To this aim, the optimized geometry of the POM^{hyd} and the most probable conformer structure were used.

The results of the quantum calculations are reported in Tables 2 and 3. The first value, in Table 2, is referred to the adduct, the atoms chosen to bond with the surfactant were the freest oxygen atoms of the hydrated nanoparticle; i.e., no water molecule directly connected with them in the optimized geometry of POM^{hyd}. Conversely, in the $(PMo_{12}O_{40})^{hyd}\cdots H_2O\cdots AUTMAB_1$ and $Br^{hyd}\cdots H_2O\cdots AUTMAB_1$, the atoms chosen were an oxygen POM^{hyd} directly bonded with a water molecule, that in turn is linked with a hydrogen atom of the surfactant's methyl group; i.e., the water molecule is considered a bridge between POM and the polar head, as shown in Figures 6 and 7 (as regards the bromide). It is worth noting that these configurations (water as a bridge) as well as the aforementioned direct link are only referred to the starting geometries used for the subsequent quantum optimizations. In fact, the interaction energies, as reported in Table 1, were calculated by using the optimized geometries in which the water molecules, both in the direct and indirect linkages, have moved. The use of two starting geometries is used only to understand how these influence the short-range interaction energies. Moreover, in the $(PMo_{12}O_{40})^{hyd}\cdots AUTMAB_3$ and $(PMo_{12}O_{40})^{hyd}\cdots AUTMAB_1$ adducts, the maximum and minimum numbers of noncovalent interactions between the surfactants and the antimicrobial particle are considered, respectively. The number of surfactants which coordinate the polyanion determines the total charge of the adduct. Hence, the $(PMo_{12}O_{40})^{hyd}\cdots AUTMAB_3$ adduct has a total charge equal to 0, whereas the total charge of the $(PMo_{12}O_{40})^{hyd}\cdots AUTMAB_1$ is equal to −2. The Na^+ ions, in solution, counterbalance the charge of the last adduct.

Table 2. Short-Range Noncovalent Interaction Energies Involved in the Anionic Exchange

adduct	total charge	ΔE_{int} (kcal/mol)
$(PMo_{12}O_{40})^{hyd}\cdots AUTMAB_3$	0	−324.81
$(PMo_{12}O_{40})^{hyd}\cdots AUTMAB_1$	−2	−112.50
$(PMo_{12}O_{40})^{hyd}\cdots H_2O\cdots AUTMAB_1$	−2	−119.98
$Br\cdots AUTMAB_1$	0	−90.62
$Br^{hyd}\cdots H_2O\cdots AUTMAB_1$	0	−85.16

Table 3. Anion Solvation Free Energies

molecule	ΔG_{sol} (kcal/mol)
$(PMo_{12}O_{40})^{-3}$	−226.08
Br^- [a]	−56.81

[a]Considering the first solvation shell Br^- ($5H_2O$) in the most stable configuration.

energy associated with the interaction among three polar heads of surfactants and the polyanion, as shown in Figure 5. The subsequent energies are instead referred to the linkage between one surfactant molecule and the POM^{hyd}, by using two different starting structures. Precisely, in the $(PMo_{12}O_{40})^{hyd}\cdots AUTMAB_1$ adduct, the atoms chosen to bond with the surfactant were the freest oxygen atoms of the hydrated nanoparticle; i.e., no water molecule directly connected with them in the optimized geometry of POM^{hyd}. Conversely, in the $(PMo_{12}O_{40})^{hyd}\cdots H_2O\cdots AUTMAB_1$ and $Br^{hyd}\cdots H_2O\cdots AUTMAB_1$, the atoms chosen were an oxygen POM^{hyd} directly bonded with a water molecule, that in turn is linked with a hydrogen atom of the surfactant's methyl group; i.e., the water molecule is considered a bridge between POM and the polar head, as shown in Figures 6 and 7 (as regards the bromide). It is worth noting that these configurations (water as a bridge) as well as the aforementioned direct link are only referred to the starting geometries used for the subsequent quantum optimizations. In fact, the interaction energies, as reported in Table 1, were calculated by using the optimized geometries in which the water molecules, both in the direct and indirect linkages, have moved. The use of two starting geometries is used only to understand how these influence the short-range interaction energies. Moreover, in the $(PMo_{12}O_{40})^{hyd}\cdots AUTMAB_3$ and $(PMo_{12}O_{40})^{hyd}\cdots AUTMAB_1$ adducts, the maximum and minimum numbers of noncovalent interactions between the surfactants and the antimicrobial particle are considered, respectively. The number of surfactants which coordinate the polyanion determines the total charge of the adduct. Hence, the $(PMo_{12}O_{40})^{hyd}\cdots AUTMAB_3$ adduct has a total charge equal to 0, whereas the total charge of the $(PMo_{12}O_{40})^{hyd}\cdots AUTMAB_1$ is equal to −2. The Na^+ ions, in solution, counterbalance the charge of the last adduct.

The interaction energies of Table 2 show that both $(PMo_{12}O_{40})^{hyd}\cdots AUTMAB_3$ and $(PMo_{12}O_{40})^{hyd}\cdots AUTMAB_1$ adducts interact with the surfactant molecules more effectively than the Br ion$^-$. The starting geometries do not affect this trend. However, this comparison does not take into account the solvation of ions. Thus, for a correct analysis, the solvation energies must be considered. The energy balance between ΔE_{int} and ΔE_{sol}, shown in Table 2, provides, therefore, information on the relative stability of the ions. The energy balance shows that, for the $(PMo_{12}O_{40})^{hyd}\cdots AUTMAB_1$ or $(PMo_{12}O_{40})^{hyd}\cdots H_2O\cdots AUTMAB_1$ adducts, i.e., considering a low density of surfactant on the polymeric surface, there is no net energy gain with respect to the hydrated POM. This means that the nanoparticle is more stable in water than attached to just one surfactant independent of the type of noncovalent short-range interaction. Instead, the energy balance, referred to as the $(PMo_{12}O_{40})^{hyd}\cdots AUTMAB_3$ adduct, shows that in this case there is a net energy gain; that is, the POM interacting with three surfactants is more stable with respect to the hydrated in the solvent bulk. As a result, with a high density of surfactant molecules on the polymeric surface, the nanoparticle is likely to be absorbed. However, this energy's balance has to be compared with the balance referred to the bromide. The difference between ΔE_{int} and ΔE_{sol} for the $(PMo_{12}O_{40})^{hyd}\cdots AUTMAB_3$ adduct is equal to −98.73 (kcal/mol), whereas the same difference referred to the $Br\cdots AUTMAB_1$ adduct is equal to −33.81 (kcal/mol). This value, nevertheless, is related to the exchange of a single Br^- ion; therefore, it cannot be compared with the energy's difference associated with the $(PMo_{12}O_{40})^{hyd}\cdots AUTMAB_3$ anion. It must be multiplied by 3 because every POM particle should break three interactions between Br^- and surfactant. Thus, the final Br energy's balance is −101.43 (kcal/mol). These two balances are comparable within the limits of calculation error. In conclusion, there is no net energy gain if three Br^- ions are exchanged with a POM nanoparticle.

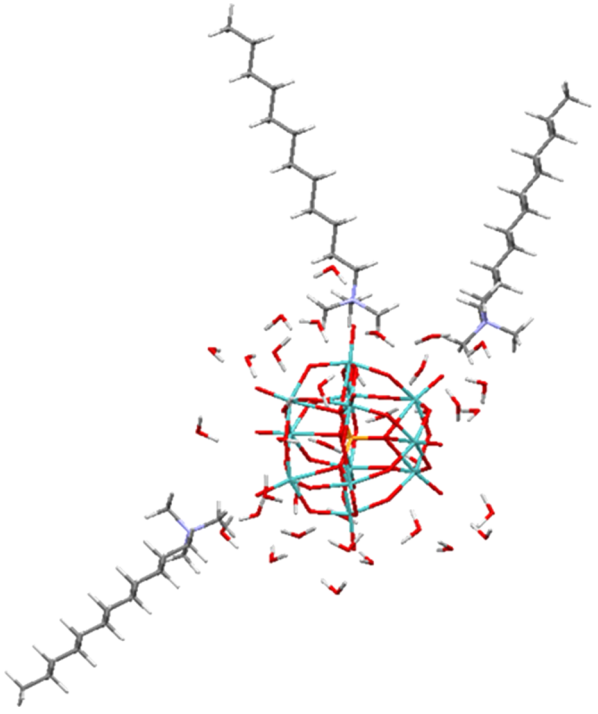

Figure 5. $(PMo_{12}O_{40})^{hyd}\cdots AUTMAB_3$ nanosized adduct formed by three surfactant molecules (ligands) and POM^{hyd}.

dx.doi.org/10.1021/jp411401v | J. Phys. Chem. B 2014, 118, 2396−2404

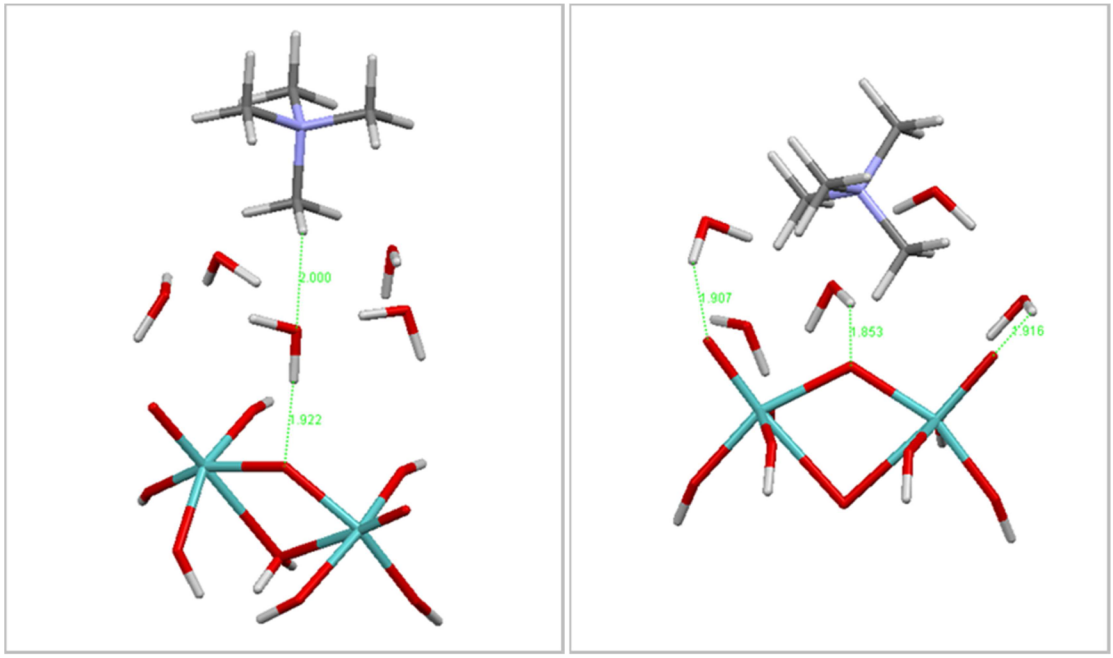

Figure 6. Initial (a) and DFT optimized geometries (b) of a POM model and a surfactant polar head. The bridge water molecule is considered in the initial geometry.

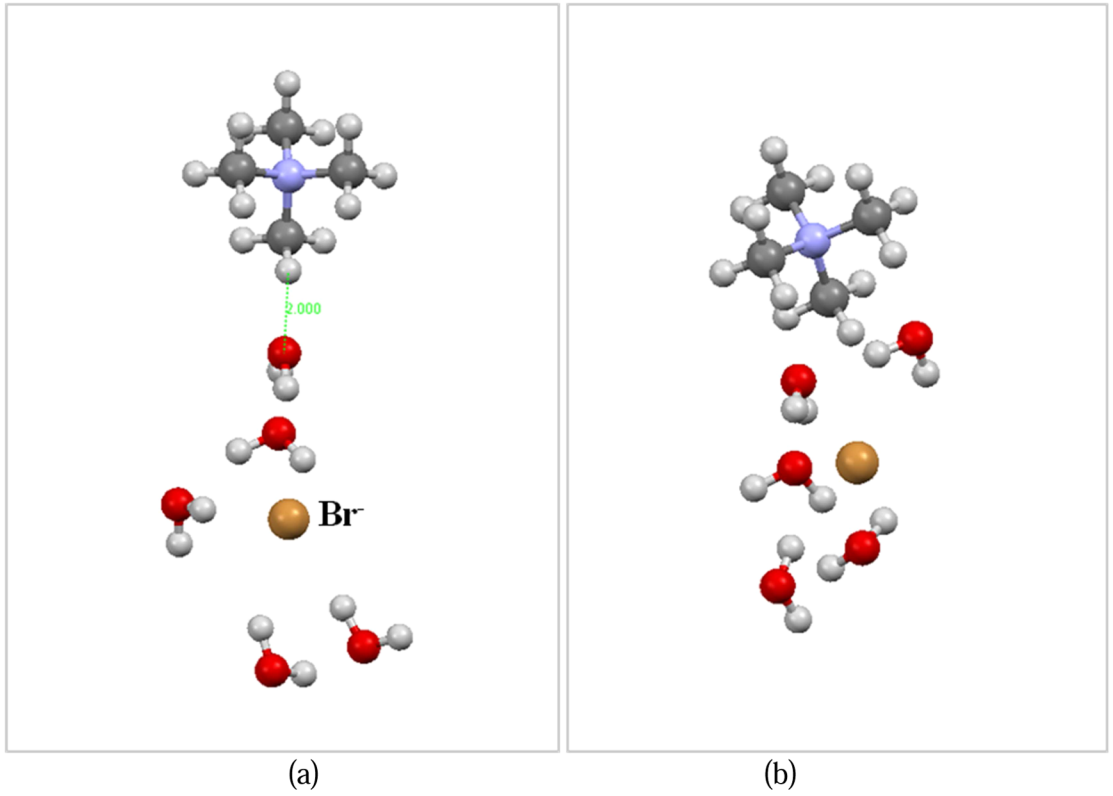

Figure 7. Initial (a) and DFT optimized geometries (b) of a surfactant polar head and Br^- ion. The bridge water molecule is considered in the initial geometry.

In these balances, the energy required to rearrange the water molecules around the POM's particle and Br^- should be considered. The assessment of this quantity through a pure quantum mechanics approach is very difficult, and it would be inaccurate, as it depends on a large time−space scale. In any case, this energy should be provided to the nanoparticle to reorganize the surrounding water molecules from the non-interacting hydrated POM (shown in Figure 4b) to the interacting POM^{hyd} structure, as shown in Figure 5, at least as regards the optimized water molecules close to the interaction

dx.doi.org/10.1021/jp411401v | J. Phys. Chem. B 2014, 118, 2396−2404

sites. Thus, the $(PMo_{12}O_{40})^{hyd}\cdots AUTMAB_3$ energy balance (i.e., −98.73 (kcal/mol)) should be reduced by the energy required to reorganize the water molecules when the nanoparticle interacts with surfactants. Nevertheless, this energy was estimated by using the optimized water geometries obtained by utilizing the models shown in Figure 6b and Figure 7b as regards the bromide. The energy required to move the water molecules was evaluated as the difference between the energy, associated with the noninteracting POM^{hyd} (Figure 4b) and the interacting POM^{hyd} energy, i.e., the energy of the nanoparticle reported in Figure 5. The positions of five water molecules, i.e., those involved in the $(PMo_{12}O_{40})^{hyd}\cdots H_2O\cdots AUTMAB_1$ interaction, were optimized, along with the surfactant polar head, by using the aforementioned model. This energy difference is 38.55 (kcal/mol). Hence, by considering the energies required to move the water molecules around the POM and Br^- ion (i.e., 2.75 (kcal/mol)), although evaluated in an approximate way, the balance is unfavorable for the POM either considering high or low density of surfactant. Though the maximum number of noncovalent interactions between surfactant and $[PMo_{12}O_{40}]^{3-}$ is considered, the computed energy gain is not so large to compensate for the energy required to shift the Br^- from the surfactant's polar head. From a macroscopic point of view, this means that the bromide−POM exchange is unfavorable or forbidden.

In order to validate this theoretical conclusion, the extent of the ionic exchange was assessed by Br^- anion gravimetrical analysis, as previously described in section 2.2. The concentrations of Br^-, released in the aqueous phase, are expressed as a function of the time and relating to the initial amount of bromide used in the PBM membrane preparation (Figure 8). As evident in Figure 8, the anionic exchange took

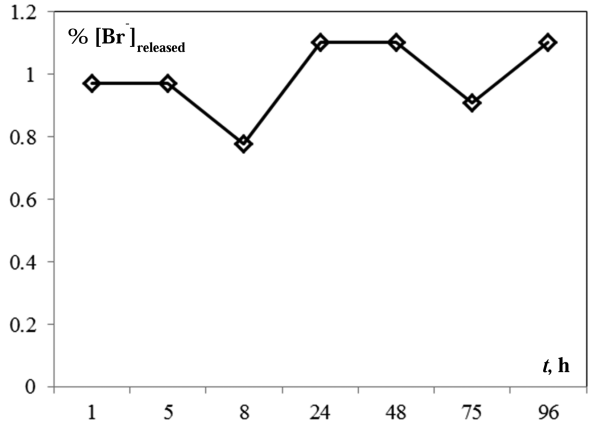

Figure 8. Relative concentrations of Br^- ion (%) released in the POM solution with respect to the time.

place during the first hour of the experiment. In fact, the percentage of the released bromide reaches a constant value, ca. 1%, after the first hour and it remains constant, within the uncertainty of measurements, for the whole period of the experiment. Moreover, it remained practically unchanged until 96 h. Another important aspect to be observed is related to the concentration of the reagents involved in the exchange process. In particular, the millimoles of starting bromide are in large excess (i.e., 2.46 mmol) compared to those of POM (i.e., 0.096 mmol). Nevertheless, the millimoles of bromide detected at the end of the process (i.e., after 96 h) are just 0.024 mmol. This value is a quarter of the milimoles of POM dissolved at the beginning of the experiment. This means that most of the POM remained in solution, confirming that the exchange is not favored. It is worth noting that a low concentration of POM was used in the analytical measurements to avoid the smallest precipitation of nanoparticles as sodium salt. Thus, the agreement between the theoretical conclusion and experimental data was remarkable. In addition, the exchange process was measured considering the PBM membrane submerged in the POM solution, as shown in Figure 2 at constant room temperature and without water flow. Under these conditions, physical adsorption of POM should be excluded by comparing the effective diameter of the POM^{hyd}, i.e., 2.36 nm, evaluated by a homemade algorithm[49] and the average pore size of the membrane of about 20 nm, measured by means of a capillary flow porometer Mod. 1500AEXL (USA) PMI.

5. CONCLUSION

Noncovalent interactions between the Keggin polyoxometalate, $[PMo_{12}O_{40}]^{3-}$, Br, and AUTMAB surfactants were evaluated in the frame of density function theory. In addition, the solvation energies of the anions were evaluated at the same level of theory. Energy balances were theoretically assessed in order to predict a probable exchange between bromide and $[PMo_{12}O_{40}]^{3-}$ on the polymeric surface. The quantum calculations predict that there is no net energy gain if the Br^- ion is exchanged with POM^{hyd}. This is evident when a low density of surfactant is considered on the polymeric surface. Instead, for high surfactant density, the energy loss due to this exchange is less marked. However, if the energy involved in the rearrangement of the water molecules, around the POM, is also considered, the balance is still unfavorable for the $[PMo_{12}O_{40}]^{3-}$ anion exchange. In order to verify this theoretical prediction, gravimetrical analysis of the Br^- anion was carried out by using a homemade polymeric membrane with controlled concentrations of all components. The agreement between the theoretical conclusion and experimental data was remarkable. In fact, this analysis showed that the exchange takes place in a very low extent. Then, this theoretical and experimental study is important because it helps to select tailored nanosized particles and polymer functionality, through an *ab initio* methodology free from any adjustable parameter, in order to optimize the exchange between ions and to improve the polymer surface properties.

AUTHOR INFORMATION

Corresponding Author

*Phone: +39 (0984) 492080. Fax: +39 (0984) 402103. E-mail: g.deluca@itm.cnr.it. Homepage: www.itm.cnr.it.

Notes

The authors declare no competing financial interest.

ACKNOWLEDGMENTS

The research leading to these results has received funding from the European Community's Seventh Framework Programme BioNexGen (Grant agreement no. CP-FP 246039-2) EU FP/ project. The authors are grateful to CINECA for the use of High Performance Computers.

REFERENCES

(1) Berndt, E.; Behnke, S.; Dannehl, A.; Gajda, A.; Wingender, J.; Ulbricht, M. Functional coatings for anti-biofouling applications by

surface segregation of block copolymer additives. *Polymer* **2010**, *51*, 5910−5920.
(2) Berndt, E.; Behnke, S.; Ulbricht, M. Influence of alkyl chain length and molecular weight on the surface functionalization via adsorption/entrapment with biocidal cationic block copolymers. *Eur. Polym. J.* **2011**, *47*, 2379−2390.
(3) Borcherding, H.; Hicke, H. G.; Jorcke, D.; Ulbricht, M. Surface functionalized microfiltration membranes for affinity separation. *Desalination* **2002**, *149*, 297−302.
(4) Urch, H.; Geismann, C.; Ulbricht, M.; Epple, M. Deposition of functionalized calcium phosphate nanoparticles on functionalized polymer surfaces. *Materialwiss. Werkstofftech.* **2006**, *37*, 422−425.
(5) Peeva, P. D.; Palupi, A. E.; Ulbricht, M. Ultrafiltration of humic acid solutions through unmodified and surface functionalized low-fouling polyethersulfone membranes−Effects of feed properties, molecular weight cut-off and membrane chemistry on fouling behavior and cleanability. *Sep. Purif. Technol.* **2011**, *81*, 124−133.
(6) Hassan, N.; Bahners, T.; Wego, A.; Gutmann, J. S.; Ulbricht, M. Surface modification of poly(ethylene terephthalate) fabric via photochemical reaction of dimethylaminopropyl methacrylamide. *Appl. Surf. Sci.* **2012**, *259*, 261−269.
(7) Fukuda, N.; Yamase, T. In vitro antibacterial activity of vanadyl compounds against Streptococcus pneumoniae. *Biol. Pharm. Bull.* **1997**, *20*, 927−930.
(8) Yang, F.-C.; Wu, K.-H.; Lin, W.-P.; Hu, M.-K. Preparation and antibacterial efficacy of bamboo charcoal/polyoxometalate biological protective material. *Microporous Mesoporous Mater.* **2009**, *118*, 467−472.
(9) Wu, K. H.; Yu, P. Y.; Yang, C. C.; Wang, G. P.; Chao, C. M. Preparation and characterization of polyoxometalate-modified poly-(vinyl alcohol)/polyethyleneimine hybrids as a chemical and biological self-detoxifying material. *Polym. Degrad. Stab.* **2009**, *94*, 1411−1418.
(10) Kong, Y.; Pan, L.; Peng, J.; Xue, B.; Lu, J.; Dong, B. Preparation and antibacterial activity of nanorod-amino acid polyoxometalates. *Mater. Lett.* **2007**, *61*, 2393−2397.
(11) Carraro, M.; Sartorel, A.; Ibrahim, M.; Nsouli, N.; Jahier, C.; Nlate, S.; Kortz, U.; Bonchio, M. In *Innovative Catalysis in Organic Synthesis Oxidation, Hydrogenation, and C-X Bond Forming Reactions*; Andersson, P., Ed.; Wiley-VCH: Weinheim, Germany, 2012; pp 1−25.
(12) Weinstock, I. A. Homogeneous-Phase Electron-Transfer Reactions of Polyoxometalates. *Chem. Rev.* **1998**, *98*, 113−170.
(13) Neumann, R.; Khenkina, A. M. Molecular oxygen and oxidation catalysis by phosphovanadomolybdates. *Chem. Commun.* **2006**, 2529−2538.
(14) Rhule, J. T.; Hill, C. L.; Judd, D. A.; Schinazi, R. F. Polyoxometalates in Medicine. *Chem. Rev.* **1998**, *98*, 327−357.
(15) Figoli, A. Synthesis of nanostructured mixed matrix membrane for facilitated gas separation. Ph.D. thesis. ISBN 90-365-1673-0.
(16) Zhou, N.; Bates, F. S.; Lodge, T. P. Mesoporous Membrane Templated by a Polymeric Bicontinuous Microemulsion. *Nano Lett.* **2006**, *6* (10), 2354−2357.
(17) Chieng, T. H.; Gan, L. M.; Teot, W. K. Porous polymeric membranes by bicontinuous microemulsion polymerization: effect of anionic and cationic surfactants. *Polymer* **1996**, *37*, 5917−5925.
(18) Gomez-Cisneros, M.; Lopez, R. G.; Peralta, R. D.; Cesteros, L. C.; Katime, I.; Mendizabal, E.; Puig, J. E. Polymerization of vinyl acetate in microemulsions stabilized with dodecyltrimethylammonium bromide and cetyltrimethylammonium bromide. *Polymer* **2002**, *43*, 2993−2999.
(19) Gan, L. M.; Li, T. D.; Chew, C. H.; Teo, W. K. Microporous Polymeric Materials from Polymerization of Zwitterionic Micro-emulsions. *Langmuir* **1995**, *11*, 3316−3320.
(20) Li, T. D.; Gan, L. M.; Chew, C. H.; Teo, W. K.; Gan, L. H. Preparation of Ultrafiltration Membranes by Direct Microemulsion Polymerization Using Polymerizable Surfactants. *Langmuir* **1996**, *12*, 5863−5868.
(21) De Luca, G.; Donato, L.; García Del Blanco, S.; Tasselli, F.; Drioli, E. On the Cause of Controlling Affinity to Small Molecules of Imprinted Polymeric Membranes Prepared by Noncovalent Approach: A Computational and Experimental Investigation. *J. Phys. Chem. B* **2011**, *115*, 9345−9351.
(22) De Luca, G.; Gugliuzza, A.; Drioli, E. Competitive Hydrogen-Bonding Interactions in Modified Polymer Membranes: A Density Functional Theory Investigation. *J. Phys. Chem. B* **2009**, *113*, 5473−5477.
(23) Gugliuzza, A.; De Luca, G.; Tocci, E.; De Lorenzo, L.; Drioli, E. Intermolecular Interactions as Controlling Factor for Water Sorption into Polymer Membranes. *J. Phys. Chem. B* **2007**, *111*, 8868−8878.
(24) De Luca, G.; Tocci, E.; Drioli, E. Quantum and molecular mechanics calculations on modified silica nano ring. *J. Mol. Struct.* **2005**, *739*, 163−172.
(25) van der Wijst, T.; Fonseca Guerra, C.; Swart, M.; Bickelhaupt, F. M. Performance of various density functionals for the hydrogen bonds in DNA base pairs. *Chem. Phys. Lett.* **2006**, *426*, 415−421.
(26) Leng, Y. S.; Krstic, P. S.; Wells, J. C.; Cummings, P. T.; Dean, D. J. Interaction between benzenedithiolate and gold: Classical force field for chemical bonding. *J. Chem. Phys.* **2005**, *122*, 244721.
(27) Fonseca Guerra, C.; Bickelhaupt, F. M.; Snijders, J. G.; Baerends, E. J. Hydrogen Bonding in DNA Base Pairs: Reconciliation of Theory and Experiment. *J. Am. Chem. Soc.* **2000**, *122*, 4117−4128.
(28) Zhao, Y.; Truhlar, D. G. Design of Density Functionals That Are Broadly Accurate for Thermochemistry, Thermochemical Kinetics, and Nonbonded Interactions. *J. Phys. Chem. A* **2005**, *109*, 5656−5667.
(29) Chew, C. H.; Li, T. D.; Gan, L. M.; Teo, W. K. Synthesis and Polymerization of a Zwitterionic Betaine Surfactant: Acryloylundecyldimethylammonio Acetate. *J. Macromol. Sci., Part A: Pure Appl. Chem.* **1995**, *32*, 211−225.
(30) Figoli, A.; Hoinkis, J.; Gabriele, B.; De Luca, G.; Galiano, F.; Ahmed Deowan, S. Bicontinuous microemulsion polymerized coating for water treatment. Patent number: ge2013a000096. Filing date: Sept 27, 2013.
(31) Furia, E.; Napoli, A.; Tagarelli, A.; Sindona, G. Speciation of 2-hydroxybenzoic acid with Calcium(II), Magnesium(II), and Nickel(II) Cations in self-medium. *J. Chem. Eng. Data* **2013**, *58*, 1349−1353.
(32) Furia, E.; Sindona, G. Interaction of Iron(III) with 2-Hydroxybenzoic Acid in Aqueous Solutions. *J. Chem. Eng. Data* **2012**, *57*, 195−199.
(33) Hanwell, M. D.; Curtis, D. E.; Lonie, D. C.; Vandermeersch, T.; Zurek, E.; Hutchison, G. R. Avogadro: An advanced semantic chemical editor, visualization, and analysis platform. *J. Cheminf.* **2012**, *4*, 17.
(34) O'Boyle, N. M.; Banck, M.; James, C. A.; Morley, C.; Vandermeersch, T.; Hutchison, G. R. Open Babel: An open chemical toolbox. *J. Cheminf.* **2011**, *3*, 33.
(35) De Luca, G.; Arbouznikov, A.; Goursot, A.; Pullumbi, P. Quantum chemical study of low-pressure adsorption in zeolitic materials. *J. Phys. Chem. B* **2001**, *105*, 4663−4668.
(36) Lopez, X.; Nieto-Draghi, C.; Bo, C.; Avalos, J. B.; Poblet, J. M. Polyoxometalates in solution: Molecular dynamics simulations on the alpha-PW12O40(3-) Keggin anion in aqueous media. *J. Phys. Chem. A* **2005**, *109*, 1216−1222.
(37) Leroy, F.; Miró, P.; Poblet, J. M.; Bo, C.; Avalos, J. B. Keggin Polyoxoanions in Aqueous Solution: Ion Pairing and Its Effect on Dynamic Properties by Molecular Dynamics Simulations. *J. Phys. Chem. B* **2008**, *112*, 8591−8599.
(38) Miró, P.; Poblet, J. M.; Bonet Avalos, J.; Bo, C. Towards a computational treatment of polyoxometalates in solution using QM methods and explicit solvent molecules. *Can. J. Chem.* **2009**, *87*, 1296−1301.
(39) Klamt, A.; Schüürmann, G. COSMO: a new approach to dielectric screening in solvents with explicit expressions for the screening energy and its gradient. *J. Chem. Soc., Perkin Trans. 2* **1993**, *2*, 799−805.
(40) Grabowski, S. J.; Robinson, T. L.; Leszczynski, J. Strong dihydrogen bonds − ab initio and 'atoms in molecules' study. *Chem. Phys. Lett.* **2004**, *386*, 44−48.
(41) Grabowski, S. J.; Sokalski, W. A.; Leszczynski, J. How short can the H...H intermolecular contact be? New findings that reveal the

covalent nature of extremely strong interactions. *J. Phys. Chem. A* **2005**, *109*, 4331−4341.
(42) Grabowski, S. J.; Sokalski, W. A. Different types of hydrogen bonds − correlation analysis for interaction energy components. *J. Phys. Org. Chem.* **2005**, *18*, 779−784.
(43) Gora, W. R.; Grabowski, S. J.; Leszczynski, J. Unique features of the resonance assisted hydrogen bonds: ab initio study. *J. Phys. Chem. A* **2005**, *109*, 6397−6405.
(44) Xu, X.; Zhang, Q.; Muller, R. P.; Goddard, W. A., III. An extended hybrid density functional (X3LYP) with improved descriptions of nonbond interactions and thermodynamic properties of molecular systems. *J. Chem. Phys.* **2005**, *122*, 014105-1−014105-14.
(45) Straatsma, T. P.; Apra, E.; Windus, T. L.; Dupuis, M. E.; Bylaska, J.; de Jong, W.; Hirata, S.; Smith, D. M.; Hackler, A. M.; Pollack, T. L.; Harrison, R. J.; Nieplocha, J.; Tipparaju, V.; Krishnan, M.; Brown, E.; Cisneros, G.; Fann, G. I.; Fruchtl, H.; Garza, J.; Hirao, K.; Kendall, R.; Nichols, J. A.; Tsemekhman, K.; Valiev, M.; Wolinski, K.; Anchell, J.; Bernholdt, D.; Borowski, P.; Clark, T.; Clerc, D.; Dachsel, H.; Deegan, M.; Dyall, K.; Elwood, D.; Glendening, E.; Gutowski, M.; Hess, A.; Jaffe, J.; Johnson, B.; Ju, J.; Kobayashi, R.; Kutteh, R.; Lin, Z.; Littlefield, R.; Long, X.; Meng, B.; Nakajima, T.; Niu, S.; Rosing, M.; Sandrone, G.; Stave, M.; Taylor, H.; Thomas, G.; van Lenthe, J.; Wong, A.; Zhang, Z. *NWChem, A Computational Chemistry Package for Parallel Computers*, version 6.1.1; Pacific Northwest National Laboratory: Richland, WA, 2005.
(46) Simon, S.; Duran, M.; Dannenberg, J. J. How does basis set superposition error change the potential surfaces for hydrogen-bonded dimers? *J. Chem. Phys.* **1996**, *105*, 11024−11031.
(47) Cramer, C. J.; Truhlar, D. G. The Role of Electrostatics in Chemistry. *Theor. Chem. Acc.* **1997**, *98*, 206−211.
(48) De Luca, G.; Bisignano, F.; Paone, F.; Curcio, S. Multi-scale modeling of protein fouling in ultrafiltration process. *J. Membr. Sci.* **2014**, *452*, 400−414.
(49) Buekenhoudt, A.; Bisignano, F.; De Luca, G.; Vandezande, P.; Wouters, M.; Verhulst, K. Unravelling the solvent flux behaviour of ceramic nanofiltration and ultrafiltration membranes. *J. Membr. Sci.* **2013**, *439*, 36−47.